ChemPubSoc Europe

DOI: 10.1002/chem.202000355

CHEMISTRY A European Journal Communication

Polycycles

A Spherically Shielded Triphenylamine and Its Persistent Radical Cation

Tobias A. Schaub,[a] Theresa Mekelburg,[b] Pavlo O. Dral,[c] Matthias Miehlich,[d] Frank Hampel,[b] Karsten Meyer,[d] and Milan Kivala*[a, e]

Abstract: This work reports the design and synthesis of a sterically protected triphenylamine scaffold which undergoes one-electron oxidation to form an amine-centered radical cation of remarkable stability. Several structural adjustments were made to tame the inherent reactivity of the radical cation. First, the parent propeller-shaped triphenylamine was planarized with sterically demanding bridging units and, second, protecting groups were deployed to block the reactive positions. The efficiently shielded triphenylamine core can be reversibly oxidized at moderate potentials (+0.38 V, vs. Fc/Fc^+ in CH_2Cl_2). Spectroelectrochemistry and chemical oxidation studies were employed to monitor the evolution of characteristic photophysical features. To obtain a better understanding of the impact of one-electron oxidation on structural and electronic properties, joint experimental and computational studies were conducted, including X-ray structural analysis, electron paramagnetic resonance (EPR), and density functional theory (DFT) calculations. The sterically shielded radical cation combines various desirable attributes: A characteristic and unobstructed absorption in the visible region, high stability which enables storage for weeks without spectroscopically traceable degradation, and a reliable oxidation/re-reduction process due to effective screening of the planarized triphenylamine core from its environment.

Arylamines are ubiquitous in cutting-edge materials[1] and their applications are manifold ranging from benchmark hole-transporting materials, such as spiro-MeOTAD,[2] efficient light emitters based on thermally activated delayed fluorescence,[3] or donor components in push-pull chromophores for photovoltaics.[4] Aromatic amines are typically characterized by moderate to low oxidation potentials.[5–7] Their corresponding radical cations — if isolable as salts — have shown merit as efficient organic oxidants.[8] A paradigmatic example is the $SbCl_6^-$ salt of the tris(4-bromophenyl)amine radical cation, so-called 'magic blue' ($\mathbf{1}^{\bullet+}$), which is frequently being employed to quantitively oxidize organic, inorganic, and organometallic donors (Figure 1 a).[9] Although $\mathbf{1}^{\bullet+}$ is considered reasonably stable, it is plagued by slow decomposition, producing colored impurities

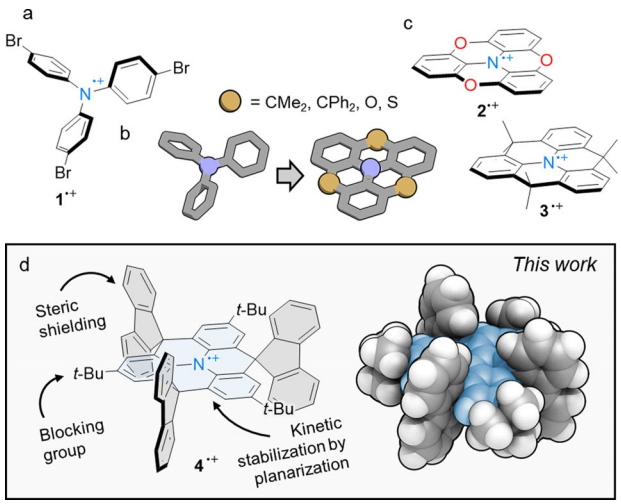

Figure 1. a) Structure of 'magic blue' radical cation $\mathbf{1}^{\bullet+}$; b) illustration of the planarization of the triphenylamine scaffold by *ortho*-bridging units, c) and representative bridged triphenylamine radical cations $\mathbf{2}^{\bullet+}$ and $\mathbf{3}^{\bullet+}$. d) Molecular design of triphenylamine radical cation $\mathbf{4}^{\bullet+}$.

[a] Dr. T. A. Schaub, Prof. Dr. M. Kivala
Institute of Organic Chemistry, Ruprecht-Karls-University Heidelberg
Im Neuenheimer Feld 270, 69120 Heidelberg (Germany)
E-mail: milan.kivala@oci.uni-heidelberg.de

[b] Dr. T. Mekelburg, Dr. F. Hampel
Department of Chemistry and Pharmacy
Friedrich-Alexander-University Erlangen-Nürnberg
Nikolaus-Fiebiger-Strasse 10, 91058 Erlangen (Germany)

[c] Prof. Dr. P. O. Dral
State Key Laboratory of Physical Chemistry of Solid Surfaces
Fujian Provincial Key Laboratory of Theoretical and Computational Chemistry, Department of Chemistry
College of Chemistry and Chemical Engineering, Xiamen University
Xiamen 361005 (P. R. China)

[d] M. Miehlich, Prof. Dr. K. Meyer
Department of Chemistry and Pharmacy, Inorganic Chemistry
Friedrich-Alexander-University Erlangen-Nürnberg
Egerlandstr. 1, 91058 Erlangen (Germany)

[e] Prof. Dr. M. Kivala
Centre for Advanced Materials (CAM)
Im Neuenheimer Feld 225, 69120 Heidelberg (Germany)

Supporting information and the ORCID identification number(s) for the author(s) of this article can be found under: https://doi.org/10.1002/chem.202000355.

— the so called 'blues brothers' — which complicate spectroscopic analysis.[10] Exploiting the rich chemistry of aromatic amines, back in the 1980s, Hellwinkel and Melan[11] reported an elegant molecular design resulting from the exhaustive introduction of bridging units at the *ortho*-position of triphenylamine, which forces the originally propeller-shaped scaffold into a virtually planar geometry (Figure 1 b).[12] Various types of bridged triphenylamines have been reported to date,[12,13] including carbonyl,[14] ether,[5,15,16] thioether,[17] dimethylmethylene,[18,19] and diphenylmethylene bridges[20] as well as triphenylamines with two fused pentagons.[21] It has been demonstrated that Hellwinkel's design principle can be adopted to stabilize *N*-centered radical cations by delocalization of the radical over the planarized π-system. Fully ether- and dimethylmethylene-bridged triphenylamine cations $\mathbf{2}^{\bullet+}$[5] and $\mathbf{3}^{\bullet+}$[15] are rare cases for which structural information based on X-ray crystallography is available (Figure 1 c). While the stabilizing effect of the ether bridges in $\mathbf{2}^{\bullet+}$ prevents follow-up reactions that may result from large spin densities at the *para*-positions,[5] radical $\mathbf{3}^{\bullet+}$ was reported to dimerize to a dicationic benzidine-like species.[15] Benchtop stable radical cations based on triphenylamine scaffold are an attractive, yet scarce class of compounds.

To further improve the stability of organic heteroatom-centered radicals, we embarked on a research program to realize bridged triphenylphosphines and -amines with sterically demanding bridging units. Our group recently showed that this strategy allows for the isolation and investigation of otherwise elusive species, such as a phosphine oxide radical anion.[22] Herein, the synthesis and detailed characterization of the first fully spiro-bridged triphenylamine **4**[23] and its persistent radical cation $\mathbf{4}^{\bullet+}$ are presented (Figure 1 d). Our strategy includes *tert*-butyl groups to block the reactive *para*-positions and bulky, rigid fluorenyl bridges, which were found to be beneficial for the materials properties of other functional arylamines.[24] Compound **4** undergoes a reversible one-electron oxidation to its radical cation $\mathbf{4}^{\bullet+}$, which is stable in solution and can be stored as a solid under ambient conditions. This remarkable stability permitted detailed investigation of the spectroscopic and structural characteristics of $\mathbf{4}^{\bullet+}$.

The synthesis of **4** is shown in Scheme 1 a. For detailed synthetic protocols we refer the reader to the Supporting Information. Starting compound **5** is available on a multigram scale by Friedel–Crafts alkylation of triphenylamine and subsequent bromination with *N*-bromosuccinimide.[10,25] Exhaustive lithium/bromine exchange of **5** with *n*BuLi at −78 °C and subsequent addition of 9-fluorenone afforded compound **6** (58% yield per functional unit). We ascribe the rather low yield to the sterically overcrowded nature of triol **6**, which is also reflected in the formation of considerable amounts of the mono- and di-substituted derivatives as the major side products. Gratifyingly, treatment of **6** with polyphosphoric acid (PPA) at 170 °C for 2 h resulted in threefold cyclization to afford **4** in high yields. Compound **4** was isolated as an air-stable, pale-yellow solid, which is well soluble in common organic solvents. It is worth mentioning that the isolation of compounds **4**–**6** does not require lengthy chromatographic purification methods and com-

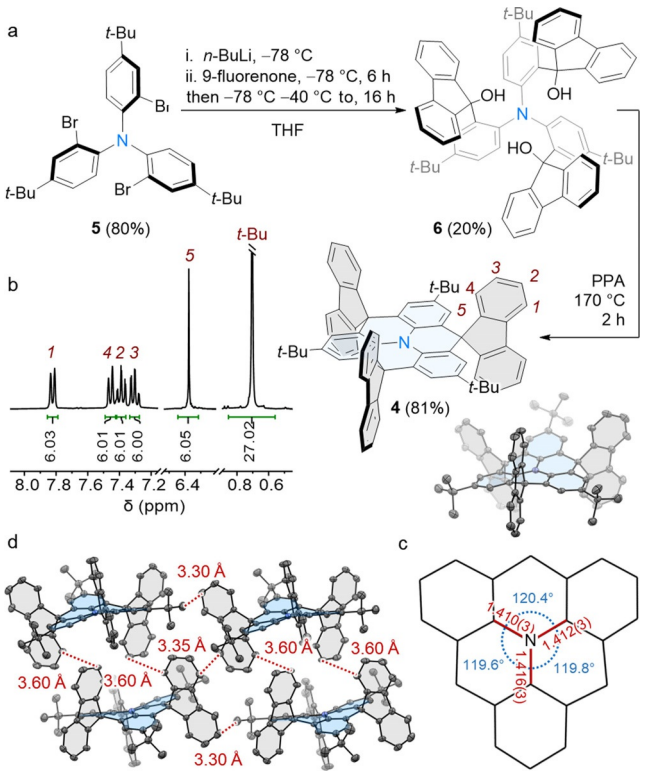

Scheme 1. a) Synthesis of target compound **4**, its b) ^{1}H NMR (300.1 MHz, CD_2Cl_2) spectrum, and c) X-ray structure along with the geometric parameters of the amine core (30% probability level, H-atoms omitted for clarity). d) Crystal packing in the solid state and short contacts.

pound **4** can be prepared within a few days from commercially available starting materials. The ^{1}H NMR spectrum of **4** features five distinct peaks in the aromatic region illustrating its overall D_{3h} symmetry in solution. Remarkably, the *tert*-butyl signals (δ 0.70 ppm) appear upfield-shifted compared to **5** (δ 1.27 ppm) and **6** (δ 1.01 ppm), which is attributed to the shielding effect of the adjacent aromatic ring current of the fluorenyl groups (Scheme 1 b; for peak assignment see the Supporting Information, Figures S24–S27). The structure of compound **4** was unambiguously determined by X-ray crystallography. Single crystals of **4** were grown by slow liquid–liquid diffusion of a CH_2Cl_2 solution layered with MeOH. The fluorenyl flanks are found to be orthogonal to the triphenylamine core, which results in an overall tripod-like shape (Scheme 1 c). The peripheral fluorenyls are bent from planarity by up to 25.5° (for the definition of the bending angle see Figure 4 b; for details see the Supporting Information, Table S1) suggesting considerable flexibility of the scaffold that leads to the deformation of the planarized triphenylamine core from ideal D_{3h} symmetry. Irrespective of the molecular distortion, the central nitrogen is not subject to any significant constraints regarding C–N bond lengths ($C–N_{av}$ 1.413(3) Å, compared 1.423(6) for NPh_3)[26] and C-N-C angles ($\Sigma_{C\text{-}N\text{-}C}$ 359.8°), thus reflecting its sp^2-hybridization to provide for efficient electronic communication with the surrounding π-systems.[27] In the crystalline state the spatial arrangement of the fluorenyl moieties in **4** leads to the formation of interdigitating dimers with multiple $C(sp^2)$-H···π (3.60 Å) interactions.

The supramolecular arrangement is largely dictated by C(sp^3)-H···π (3.30 Å), and π···π (3.35 Å) interactions (Scheme 1 d).[28]

Considering the orthogonality of the triphenylamine core and the three fluorenyl flanks, we speculated that—according to Krapp's concept of spiro-conjugation[29] — compound **4** can be regarded as four chromophoric subunits in the ground state. To prove this hypothesis, the electronic absorption and emission spectra of compound **4** were recorded in CH_2Cl_2 at room temperature (Figure 2 a). Spirocycle **4** shows two distinct

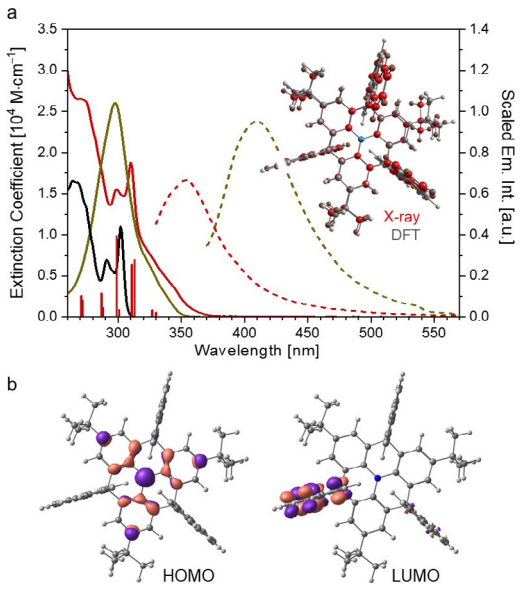

Figure 2. a) Electronic absorption (solid) and emission spectra (dashed) of compound **4** (red), its dimethylmethylene-bridged relative **3** (olive), and 9,9-dimethylfluorene (**7**, black) recorded in CH_2Cl_2 at room temperature; oscillator strengths for **4** (TD-DFT, red bars shifted by +35 nm); superimposed X-ray and DFT-optimized structures of **4** (inset); b) Kohn–Sham orbitals (0.05 $e^{1/2}$·$Bohr^{-3/2}$ isosurfaces). All calculations were performed at the ωB97X-D/def2-TZVP level of theory.

absorption bands at 310 and 299 nm accompanied by a long wavelength shoulder extending to approx. 360 nm. Comparison to the absorptions of **3** and 9,9-dimethylfluorene (**7**) suggests the low energy shoulder to originate from the triphenylamine core, whereas the transitions at 299 and 310 nm are a superimposition of the features from the triphenylamine core, and the fluorenyls. To disclose the nature of the underlying electronic transitions, DFT calculations were conducted at the ωB97X-D[30]/def2-TZVP[31] level of theory. Noticeable differences are observed for the peripheral fluorenyls between the X-ray structure of **4** and the essentially D_{3h} symmetric gas-phase DFT-optimized structure, which is ascribed to the distortion of the scaffold in the solid state; proposedly due to packing effects (Figure 2 a inset). However, in the most important geometrical features of the triphenylamine core (bond lengths and angles) the experimental and the DFT-optimized structure are in good agreement. The electronic absorption spectrum of **4** simulated with time-dependent (TD) ωB97X-D/def2-TZVP reproduced the experimentally observed trace and provides a deeper understanding of its features: The low-energy tail at 360 nm originates from two transitions with low oscillator strengths (*f*), S_1 (HOMO→LUMO+3, $f=0.02$) and S_2 (HOMO→LUMO+4, $f=0.03$), which are similar in nature to those responsible for the low-energy tail in **3** (for more details, see the Supporting Information). S_3 (HOMO→LUMO, $f=0.24$, Figure 2 b) and S_4 (HOMO→LUMO+1, $f=0.22$) are due to local excitations in **3** and are reflecting the very broad band around 320 nm. Superimposed to this band, two sharp features are found around 300 nm and 310 nm, which correspond to strong excitations S_8 (HOMO-1→LUMO+2, $f=0.34$) and S_{11}–S_{13} (various transitions HOMO−*n*→LUMO+*m*) exclusively located at the fluorene moieties. The contributions from the central triphenylamine and the peripheral fluorenyls in **4** can be clearly seen from comparison with model compounds **3** and **7**, respectively (Figure S10). However, the interaction between these structural components in **4** through spiro-conjugation leads to a clear redshift. Experimentally, compound **4** was found to be weakly emissive ($\lambda_{em}=354$ nm, $\Phi<0.03$ in CH_2Cl_2) similar to its relative **3**,[19] however, significantly blueshifted by (0.46 eV). This finding is in good qualitative agreement with the computational predictions, indicating that excitation of **4** mostly affects the triphenylamine core similarly to related compound **3**, while key bond lengths of the fluorenyl moieties remain close to those in ground-state of **7** (see the Supporting Information).

Having analyzed the fundamental photophysical properties of compound **4** we turned our attention to the study of its radical cation. Cyclic voltammetry (CV) in CH_2Cl_2 with 0.1 M nBu$_4$NPF$_6$ provided a first insight into the formation of radial cation **4**$^{\bullet+}$ (all potentials are reported vs. Fc/Fc$^+$, Table 1). A fully reversible one-electron oxidation is observed at +0.38 V. This oxidation event appeared shifted to less positive potentials as compared to the parent non-bridged NPh_3 (E_{ox} +0.53 V), which is ascribed to the efficient delocalization of the positive charge over the planarized triphenylamine core — an effect well documented for other bridged triphenylamines.[12] The stability of the radical cation allowed us to study the evolution of characteristic spectroscopic features upon oxidation. Spectroelectrochemical measurements of **4** in CH_2Cl_2 with 0.1 M nBu$_4$NPF$_6$ at +0.36 V showed a rising absorption band at 670 nm (shoulder at around 600 nm) as well as a sharp band at 369 nm (see the Supporting Information, Figure S4). The long wavelength absorption band appears slightly bathochromically shifted as compared of **3**$^{\bullet+}$ (aprrox.

Table 1. Photophysical and electrochemical data of the title compounds (for more details on the measurement conditions, see the Supporting Information).

	λ_{max} [nm][a] ε [10^4 M^{-1}cm^{-1}]	λ_{em} [nm]	Φ	E_{ox} [V]	E_{HOMO}/E_{LUMO}[d] [eV]
3	298 (2.61)	411	0.02[21]	+0.34[21]	−6.94/1.35
4	310 (1.88)	354	<0.03[b]	+0.38	−6.82/0.59

[a] 10^{-6} M in CH_2Cl_2. [b] Quantum yields determined using an integrating sphere. [c] Redox potentials from cyclic voltammetry vs. Fc/Fc$^+$ (0.1 M nBu$_4$NPF$_6$ in CH_2Cl_2, scan rate 100 mV s^{-1}). [d] DFT, ωB97X-D/def2-TZVP.

580 nm),[15] despite a similarly C(sp^3)-bridged triphenylamine core, which we ascribe to the electronic influence of the orthogonal fluorenyls as well as the *tert*-butyl groups. As a consequence, oxidation resulted in a pronounced color change from beige to deep blue as a common characteristic of various *N*-centered radicals.[5–7] The observed isosbestic point at 340 nm and the complete recovery of the initial spectrum upon reduction of the electrogenerated species suggest that radical cation **4**$^{\bullet+}$ is formed without any spectroscopically traceable side products.

To further probe the stability of radical cation **4**$^{\bullet+}$, chemical oxidation was carried out with various inorganic and organic oxidizing agents, such as $AgSbF_6$ or $B(C_6F_5)_3$, respectively (Figure 3a). In solution, deep blue radical cation **4**$^{\bullet+}$ did not show any degradation for months when kept under N_2 at 7 °C and its SbF_6^- salt — isolable as a deep blue powder in 92% yield by precipitation from hexanes — can be stored for several weeks even under ambient conditions. To monitor the progress of the reaction, a solution of compound **4** in CH_2Cl_2 was titrated with $AgSbF_6$ (0.09 equiv per addition) and the evolution of the low energy absorption bands followed by UV/Vis absorption spectroscopy (Figure 3b). Two bands emerge centered at 369 and 670 nm at the expense of the 299 and 310 nm absorptions, which is in perfect agreement with the results from spectroelectrochemistry. We find the radical cation related band at 670 nm to linearly increase with amount of oxidant added and leveling off at approx. 1.0 equiv. oxidant added, indicating complete and clean oxidation to radical cation **4**$^{\bullet+}$. TD-DFT simulation of the UV/Vis absorption spectrum of radical cation **4**$^{\bullet+}$ in vacuum reproduces the experimentally observed bands (Figure 3b and c).[32] The lowest-energy transitions with notable oscillator strengths in **4**$^{\bullet+}$ are D_4 (βHOMO-9→βLUMO, $f=0.22$) and D_5 (βHOMO-10→βLUMO, $f=0.22$) corresponding to the intense absorptions in the visible (for further transitions, see the Supporting Information, Table S7). It is worth noting that all orbitals involved in these excitations are predominantly localized on the shielded triphenylamine core, thus adding to the observed stability of **4**$^{\bullet+}$.

Single crystals of [(**4**$^{\bullet+}$)SbF_6^-] suitable for X-ray crystallographic analysis were obtained by liquid diffusion from CH_2Cl_2 and MeOH.[33] Figure 4a shows the molecular structure of the [(**4**$^{\bullet+}$)SbF_6^-] ion pair with the triphenylamine core highlighted. The overall geometry is retained upon oxidation and the triphenylamine core remains virtually planar ($\Sigma_{\angle C\text{-}N\text{-}C}$ **4**: 359.8°,

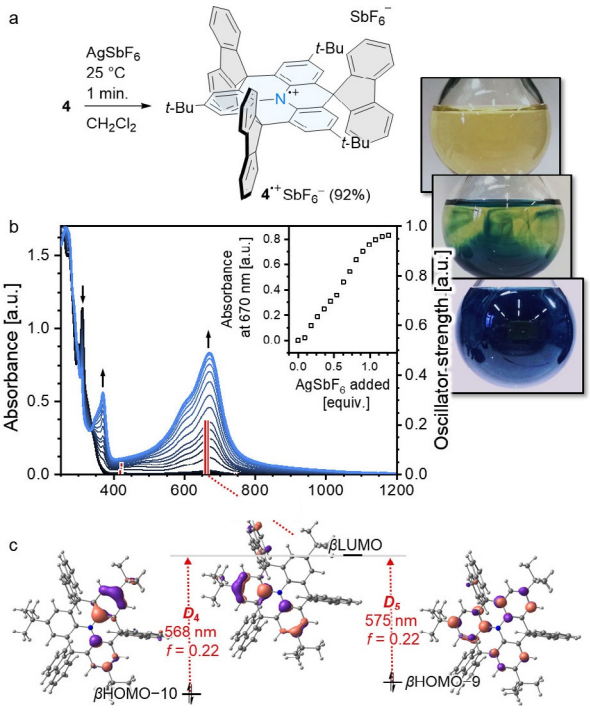

Figure 3. a) Generation of **4**$^{\bullet+}$ through chemical oxidation with $AgSbF_6$ in CH_2Cl_2; b) evolution of the UV/Vis absorption bands upon titration of **4** with $AgSbF_6$ along with the increase of the 670 nm absorption band (inset); color change upon addition of oxidant $AgSbF_6$; c) major electronic transitions (red bars shifted by +99 nm) and involved Kohn–Sham orbitals (UωB97X-D/def2-TZVP, 0.05 e$^{1/2}$·Bohr$^{-3/2}$ isosurfaces).

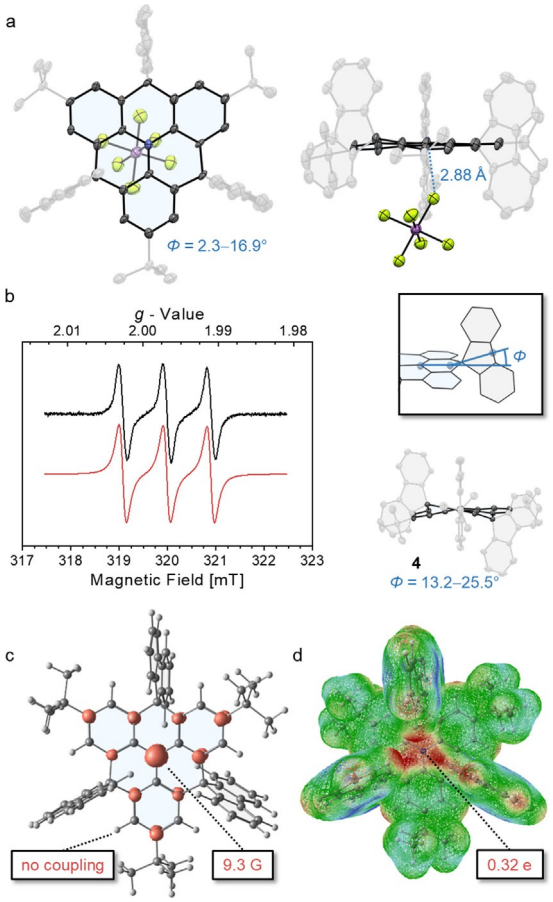

Figure 4. Study of radical cation **4**$^{\bullet+}$: a) Top and side view of the molecular X-ray structure of [(**4**$^{\bullet+}$)SbF_6^-] and its neutral analogue **4** along with the definition of the fluorenyl bending angle (30% probability level, *tert*-butyls and fluorenyls faded out for clarity; hydrogens omitted); N–C bond lengths and C-N-C angles for **4**$^{\bullet+}$: 1.397(16) Å, 1.407(17) Å, 1.433(15) Å, 121.4(9)°, 119.6(11)°, and 118.7(11)°; b) X-band EPR spectrum of [(**4**$^{\bullet+}$)SbF_6^-] (black: experiment, red: simulation); Simulation parameters: $g_{iso}=1.997$, $W_{iso}=1.34$ G, $a_N=9.13$ G (25.50 MHz); c) electronic spin-density isosurface plotted with contour value of 0.008 e Bohr^{-3} (UωB97X-D/def2-TZVP); d) molecular electrostatic potential of **4**$^{\bullet+}$ mapped on the electron density (0.006 e Bohr^{-3} isosurface, more positive potential in red, less positive in blue; 0.32 e is Mulliken charge on nitrogen atom).

$4^{\bullet+}$: 359.7°). The SbF_6^- counterion accommodates the cavity created by the fluorenyl flanks next to the positively charged triphenylamine core with short N···F distance (2.88 Å). As with other bridged triphenylamines[5–7] oxidation of **4** leads to a more rigid triphenylamine core. This structural situation is reflected by reduced bending angles of the peripheral fluorenyls in $4^{\bullet+}$ (2.3–16.9°) compared to its neutral form (13.2–25.5°), which is in good agreement with our DFT calculations predicting compound **4** to be slightly more planar in its oxidized form ($\Sigma_{\angle C\text{-}N\text{-}C}$ 360.0°) than in its neutral (356.1°) in the gas phase. In line with this finding, the EPR spectrum of $4^{\bullet+}$, recorded in CH_2Cl_2 at 293 K, exhibited a well resolved signal (Figure 4b), indicating the localization of the unpaired electron at the nitrogen center. The isotropic *g*-value, g_{iso}, was simulated to 1.997 with a hyperfine coupling constant, a_N, of 9.13 G. These values are in good agreement with the EPR spectral features reported for $2^{\bullet+}$ ($g_{iso}=2.0031$, $a_N=8.97$ G)[5] and $3^{\bullet+}$ ($g_{iso}=2.0027$, $a_N=9.40$ G).[15] In contrast to previous reports, superhyperfine coupling to *meta* protons is not observed for $4^{\bullet+}$. Calculations on radical cation $4^{\bullet+}$ were performed within the spin-unrestricted Kohn–Sham DFT formalism. The spin density (ρ) is localized on the central triphenylamine — particularly on its nitrogen center ($\rho=0.37$) and the *ortho*- ($\rho=0.09$) and *para*-carbons ($\rho=0.11$, Figure 4c). The molecular electrostatic potential plot clearly shows that $4^{\bullet+}$ carries a significant positive charge in the region near the nitrogen center, which is shielded from the environment by the bulky fluorenyl and *tert*-butyl groups (Figure 4d).

In summary, a remarkably stable molecular radical cation was made accessible in a concise synthetic strategy employing a spherically shielded, planarized triphenylamine. Specifically, *tert*-butyl groups and spiro-fluorenyl bridges were installed to protect reactive sides with large spin densities and to stabilize the positive charge of the corresponding radical cation by planarizing the triphenylamine core. Despite this extensive shielding, efficient electron abstraction can be achieved by electrochemical and chemical processes. The generated radical cation displays advantageous stability. For instance, its SbF_6^- salt could be stored for weeks under ambient conditions without spectroscopic degradation. Detailed characterization based on joint computational and experimental methods including electron paramagnetic resonance measurements and X-ray crystallography provide a clear picture of its structural and electronic attributes. Considering the intense and unobstructed absorption of the radical cation in the visible region we see potential in this compound to be a reliable redox indicator.

Acknowledgements

The authors thank Dr. Jean-Paul Gisselbrecht from the Université de Strasbourg for his help with spectroelectrochemistry measurements. For financial support T.M. thanks the Evangelisches Studienwerk Villigst. K.M. thanks the FAU Erlangen-Nürnberg for generous financial support. M.K. gratefully acknowledges funding by the Deutsche Forschungsgemeinschaft (DFG) — Project number 182849149 — SFB 953 and project number 401247651 — KI 1662/3-1. T.S. is grateful for financial support by the DFG (return scholarship — project number SCHA 2061/2-1) and the Verband der chemischen Industrie (Liebig Fellowship).

Conflict of interest

The authors declare no conflict of interest.

Keywords: bridged triphenylamines · polycyclic systems · radical cations · spirocycles

[1] a) P. Agarwala, D. Kabra, *J. Mater. Chem. A* **2017**, *5*, 1348; b) E. Moulin, J. J. Armao, N. Giuseppone, *Acc. Chem. Res.* **2019**, *52*, 975.
[2] U. Bach, D. Lupo, P. Comte, J. E. Moser, F. Weissörtel, J. Salbeck, H. Spreitzer, M. Grätzel, *Nature* **1998**, *395*, 583.
[3] a) G. Méhes, H. Nomura, Q. Zhang, T. Nakagawa, C. Adachi, *Angew. Chem. Int. Ed.* **2012**, *51*, 11311; *Angew. Chem.* **2012**, *124*, 11473; b) For a comprehensive review on thermally activated delayed fluorescence, see: Z. Yang, Z. Mao, Z. Xie, Y. Zhang, S. Liu, J. Zhao, J. Xu, Z. Chi, M. P. Aldred, *Chem. Soc. Rev.* **2017**, *46*, 915.
[4] For selected publications on photovoltaics using amine-based donors, see: a) S. Roquet, A. Cravino, P. Leriche, O. Alévêque, P. Frère, J. Roncali, *J. Am. Chem. Soc.* **2006**, *128*, 3459; b) M. Ishida, S. W. Park, D. Hwang, Y. B. Koo, J. L. Sessler, D. Y. Kim, D. Kim, *J. Phys. Chem. C* **2011**, *115*, 19343; c) Y. Hong, J.-Y. Liao, D. Cao, X. Zang, D.-B. Kuang, L. Wang, H. Meier, C.-Y. Su, *J. Org. Chem.* **2011**, *76*, 8015; d) R. Milan, G. S. Selopal, M. Cavazzini, S. Orlandi, R. Boaretto, S. Caramori, I. Concina, G. Pozzi, *Sci. Rep.* **2017**, *7*, 15675.
[5] M. Kuratsu, M. Kozaki, K. Okada, *Angew. Chem. Int. Ed.* **2005**, *44*, 4056; *Angew. Chem.* **2005**, *117*, 4124.
[6] S. Sumalekshmy, K. R. Gopidas, *Chem. Phys. Lett.* **2005**, *413*, 294.
[7] C. Quinton, V. Alain-Rizzo, C. Dumas-Verdes, F. Miomandre, G. Clavier, P. Audebert, *RSC Adv.* **2014**, *4*, 34332.
[8] N. G. Connelly, W. E. Geiger, *Chem. Rev.* **1996**, *96*, 877.
[9] a) F. A. Bell, A. Ledwith, D. C. Sherrington, *J. Chem. Soc. C* **1969**, 2719; b) M. Quiroz-Guzman, S. N. Brown, *Acta Crystallogr. Sect. C* **2010**, *66*, m171.
[10] M. R. Talipov, M. M. Hossain, A. Boddeda, K. Thakur, R. Rathore, *Org. Biomol. Chem.* **2016**, *14*, 2961.
[11] D. Hellwinkel, M. Melan, *Chem. Ber.* **1971**, *104*, 1001.
[12] N. Hammer, T. A. Schaub, U. Meinhardt, M. Kivala, *Chem. Rec.* **2015**, *15*, 1119.
[13] M. Hirai, N. Tanaka, M. Sakai, S. Yamaguchi, *Chem. Rev.* **2019**, *119*, 8291.
[14] a) J. E. Field, D. Venkataraman, *Chem. Mater.* **2002**, *14*, 962; b) H. Zhang, S. Wang, Y. Li, B. Zhang, C. Du, X. Wan, Y. Chen, *Tetrahedron* **2009**, *65*, 4455; c) H. Zhang, Y. Li, X. Wan, Y. Chen, *Chem. Phys. Lett.* **2009**, *479*, 117; d) X. Wan, H. Zhang, Y. Li, Y. Chen, *New J. Chem.* **2010**, *34*, 661; e) S. Wang, M. Kivala, I. Lieberwirth, K. Kirchhoff, X. Feng, W. Pisula, K. Müllen, *ChemPhysChem* **2011**, *12*, 1648; f) M. Kivala, W. Pisula, S. Wang, A. Mavrinskiy, J.-P. Gisselbrecht, X. Feng, K. Müllen, *Chem. Eur. J.* **2013**, *19*, 8117; g) C. Steiner, J. Gebhardt, M. Ammon, Z. Yang, A. Heidenreich, N. Hammer, A. Görling, M. Kivala, S. Maier, *Nat. Commun.* **2017**, *8*, 14765; h) A. T. Haedler, K. Kreger, A. Issac, B. Wittmann, M. Kivala, N. Hammer, J. Koehler, H.-W. Schmidt, R. Hildner, *Nature* **2015**, *523*, 196.
[15] X. Zheng, X. Wang, Y. Qiu, Y. Li, C. Zhou, Y. Sui, Y. Li, J. Ma, X. Wang, *J. Am. Chem. Soc.* **2013**, *135*, 14912.
[16] a) M. Kuratsu, S. Suzuki, M. Kozaki, D. Shiomi, K. Sato, T. Takui, T. Kanzawa, Y. Hosokoshi, X.-Z. Lan, Y. Miyazaki, A. Inaba, K. Okada, *Chem. Asian J.* **2012**, *7*, 1604; b) S. Suzuki, A. Nagata, M. Kuratsu, M. Kozaki, R. Tanaka, D. Shiomi, K. Sugisaki, K. Toyota, K. Sato, T. Takui, K. Okada, *Angew. Chem. Int. Ed.* **2012**, *51*, 3193; *Angew. Chem.* **2012**, *124*, 3247.
[17] a) S. Menichetti, S. Cecchi, P. Procacci, M. Innocenti, L. Becucci, L. Franco, C. Viglianisi, *Chem. Commun.* **2015**, *51*, 11452; b) G. Lamanna, C. Faggi, F. Gasparrini, A. Ciogli, C. Villani, P. J. Stephens, F. J. Devlin, S. Menichetti, *Chem. Eur. J.* **2008**, *14*, 5747; c) B. D. Gliemann, A. G. Petrovic, E. M. Zolnhofer, P. O. Dral, F. Hampel, G. Breitenbruch, P. Schulze, V. Ra-

ghavan, K. Meyer, P. L. Polavarapu, N. Berova, M. Kivala, *Chem. Asian J.* **2017**, *12*, 31.

[18] a) D. Hellwinkel, M. Melan, *Chem. Ber.* **1974**, *107*, 616; b) M. Bieri, S. Blankenburg, M. Kivala, C. A. Pignedoli, P. Ruffieux, K. Müllen, R. Fasel, *Chem. Commun.* **2011**, *47*, 10239; c) Z. Fang, V. Chellappan, R. D. Webster, L. Ke, T. Zhang, B. Liu, Y.-H. Lai, *J. Mater. Chem.* **2012**, *22*, 15397; d) Z. Fang, X. Zhang, Y. Hing Lai, B. Liu, *Chem. Commun.* **2009**, 920; e) S. Paek, N. Cho, S. Cho, J. K. Lee, J. Ko, *Org. Lett.* **2012**, *14*, 6326; f) P. Qin, S. Paek, M. I. Dar, N. Pellet, J. Ko, M. Grätzel, M. K. Nazeeruddin, *J. Am. Chem. Soc.* **2014**, *136*, 8516; g) C. Steiner, B. D. Gliemann, U. Meinhardt, M. Gurrath, B. Meyer, M. Kivala, S. Maier, *J. Phys. Chem. C* **2015**, *119*, 25945.

[19] F. Schlütter, F. Rossel, M. Kivala, V. Enkelmann, J.-P. Gisselbrecht, P. Ruffieux, R. Fasel, K. Müllen, *J. Am. Chem. Soc.* **2013**, *135*, 4550.

[20] a) Z. Jiang, Y. Chen, C. Yang, Y. Cao, Y. Tao, J. Qin, D. Ma, *Org. Lett.* **2009**, *11*, 1503; b) Z. Jiang, T. Ye, C. Yang, D. Yang, M. Zhu, C. Zhong, J. Qin, D. Ma, *Chem. Mater.* **2011**, *23*, 771; c) C. Liu, Y. Li, Y. Zhang, C. Yang, H. Wu, J. Qin, Y. Cao, *Chem. Eur. J.* **2012**, *18*, 6928; d) F. Wu, Lee, L. T. Lin, J. Liu, S. Zhao, T. Chen, M. Wang, C. Zhong, L. Zhu, *Synth. Met.* **2015**, *205*, 70; e) F. Wu, S. Zhao, Lee, L. T. Lin, M. Wang, T. Chen, L. Zhu, *Tetrahedron Lett.* **2015**, *56*, 1233.

[21] N. Deng, G. Zhang, *Org. Lett.* **2019**, *21*, 5248.

[22] T. A. Schaub, E. M. Zolnhofer, D. P. Halter, T. E. Shubina, F. Hampel, K. Meyer, M. Kivala, *Angew. Chem. Int. Ed.* **2016**, *55*, 13597; *Angew. Chem.* **2016**, *128*, 13795.

[23] This compound has been theoretically proposed earlier, see: Z. L. Zhang, L.-Y. Zou, A.-M. Ren, C.-G. Min, Y. Sun, Y.-F. Liu, *Int. J. Quantum Chem.* **2012**, *112*, 1473.

[24] a) M. Numata, T. Yasuda, C. Adachi, *Chem. Commun.* **2015**, *51*, 9443; b) T.-A. Lin, T. Chatterjee, W.-L. Tsai, W.-K. Lee, M.-J. Wu, M. Jiao, K.-C. Pan, C.-L. Yi, C.-L. Chung, K.-T. Wong, C.-C. Wu, *Adv. Mater.* **2016**, *28*, 6976; c) P. K. Samanta, D. Kim, V. Coropceanu, J.-L. Brédas, *J. Am. Chem. Soc.* **2017**, *139*, 4042.

[25] D. Vak, J. Jo, J. Ghim, C. Chun, B. Lim, A. J. Heeger, D.-Y. Kim, *Macromolecules* **2006**, *39*, 6433.

[26] E. Martin, C. R. Pulham, S. Parsons, CCDC 660790*: Experimental Crystal Structure Determination*, Cambridge Crystallographic Data Centre, The Cambridge Crystallographic Data Centre.

[27] a) K. Sakanoue, M. Motoda, M. Sugimoto, S. Sakaki, *J. Phys. Chem. A* **1999**, *103*, 5551; b) P. O. Dral, M. Kivala, T. Clark, *J. Org. Chem.* **2013**, *78*, 1894.

[28] a) L. M. Salonen, M. Ellermann, F. Diederich, *Angew. Chem. Int. Ed.* **2011**, *50*, 4808; *Angew. Chem.* **2011**, *123*, 4908; b) S. Grimme, *Angew. Chem. Int. Ed.* **2008**, *47*, 3430; *Angew. Chem.* **2008**, *120*, 3478.

[29] A. Schweig, U. Weidner, D. Hellwinkel, W. Krapp, *Angew. Chem. Int. Ed. Engl.* **1973**, *12*, 310; *Angew. Chem.* **1973**, *85*, 360.

[30] J.-D. Chai, M. Head-Gordon, *Phys. Chem. Chem. Phys.* **2008**, *10*, 6615.

[31] F. Weigend, R. Ahlrichs, *Phys. Chem. Chem. Phys.* **2005**, *7*, 3297.

[32] We would like to specifically point out that UV/Vis spectrum simulation of radical cation $\mathbf{4}^{\bullet+}$ was performed in vacuum. The large shift of approx. 100 nm may be a result of the simplified picture we provide, not taking into account the — proposedly significant — effects of the counterion.

[33] For the sake of conciseness only one of the two independent molecules of **4** is discussed in here. For more details, see the Supporting Information.

Manuscript received: January 21, 2020
Accepted manuscript online: January 23, 2020
Version of record online: February 21, 2020

